MRS Advances

Elucidation of the growth mechanism of MoS_2 during the CVD process

Sajeevi S Withanage[1,2], Mike Lopez[2], Wasee Sameen[2], Vanessa Charles[2], Saiful I Khondaker[1,2,3]

[1] *Department of Physics, University of Central Florida, Orlando, FL 32816, United States*

[2] *NanoScience Technology Center, University of Central Florida, Orlando, FL 32816, United States*

[3] *Department of Electrical & Computer Engineering, University of Central Florida, Orlando, FL 32816, United States*

ABSTRACT

Chemical vapor deposition (CVD) growth of two-dimensional molybdenum disulfide (MoS_2) using molybdenum trioxide (MoO_3) and sulfur (S) powder often results in intermediate molybdenum oxy-sulfide ($MoOS_2$) species along with MoS_2 due to a lack of control over the vapor pressure required for the clean growth. Much effort has been devoted in understanding and controlling of these intermediate $MoOS_2$ specifies. Here, we show that with a second step sulfurization at moderate temperatures, these $MoOS_2$ crystals can be transformed to monolayer MoS_2 crystals. Scanning electron microscopy, Raman and photoluminescence spectroscopy and atomic force microscopy characterization carried out before and after re-sulfurization confirm the monolayer MoS_2 growth via this route. This study shows that $MoOS_2$ formed at the intermediate state can be successfully recycled to MoS_2.

INTRODUCTION

Two dimensional transition metal dichalcogenides (TMDCs) has received a great deal of interest in the recent times due to their exciting properties such as layer dependent band structure, emergent photoluminescence[1, 2] and appreciable charge mobility[3].

Being the most studied member in the TMDC family, molybdenum disulfide (MoS_2) has shown many interesting applications in the fields of electronics and optoelectronics[4-8]. Due to this rapidly increasing interest in device applications, large scale scalable synthesis of MoS_2 beyond micromechanical exfoliation is highly desirable[9].

Chemical vapor deposition (CVD) based co-evaporation of molybdenum (Mo) and solfur (S) precursors is a popular method for the single crystal growth of MoS_2[10]. Molybdenum trioxide (MoO_3) powder is widely used as the Mo source while sulfur powder is used as S source for this synthesis. Reaction mechanism of MoO_3 with S suggests that a tight control of uniform vapor pressure in gas phase is highly desirable for clean and reproducible growth of MoS_2 growth[11]. However, such a control of uniform vapor pressure turned out to be very challenging resulting in a growth of oxide/oxysulfide (MoO_2/$MoOS_2$) species along with MoS_2[12, 13]. Sulfur deficiency can terminate the reaction by depositing molybdenum oxysulfides ($MoOS_2$) on the substrate. Even with excess amount of initial loading, sulfur deficiency can locally occur due to relatively high MoO_3 vapor pressure at some regions since the evaporation of MoO_3 powder is uneven. In this paper, we demonstrate a route for the synthesis of monolayer MoS_2 crystal via re-sulfurization of intermediate $MoOS_2$ species. Detailed scanning electron microscopy (SEM), Raman, photoluminescence (PL) spectroscopy and atomic force microscopy (AFM) characterization carried out before and after re-sulfurization confirm the monolayer MoS_2 growth via this route.

EXPERIMENTAL DETAILS

Growth process:

Synthesizing MoS_2/$MoOS_2$ crystals: We synthesized $MoOS_2$/MoS_2 in a home-built CVD system. A schematic diagram of our experimental setup is shown in figure 1a). Si/SiO_2 substrates with 250 nm thick oxide layer were used as the growth substrates. The substrate was cleaned via sonication in acetone for 5 min followed by sonication in IPA

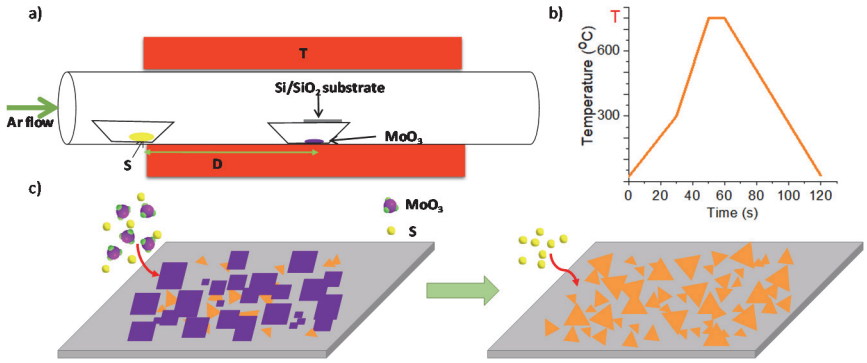

Figure 1. a) Schematic representation of the experimental setup for $MoOS_2$/MoS_2 growth. b) Temperature profile at the center of the furnace. The setpoint temperature is shown as T. c) A cartoon that showing $MoOS_2$/MoS_2 growth on the substrate and their further sulfurization.

for 5min, DI rinse and 10 min mild oxygen plasma treatment. A 0.5 mg MoO_3 powder (99.5%, Sigma Aldrich) placed in a ceramic boat, substrates were placed on the same boat facing down toward the MoO_3 powder and placed at the center of the furnace. Ceramic crucible containing 300 mg of S powder (99.5%, Sigma Aldrich) was loaded in to a 2-inch

quartz tube placed in the edge of the tube furnace (Across International STF 1200 C Tube Furnace) at a distance 15 cm away from the MoO_3 source that was placed at the center of the furnace. Argon (Ar) gas (99.995% purity) was used as the carrier gas. Temperature of the furnace was raised to 300 ^{0}C in 30 min, then raised to the setpoint value (T) of 750 ^{0}C in 20 min and hold for 10 min (dwell time). After the dwell time, the furnace was allowed to cool down to room temperature naturally. High flow of gas was passed before heating up the furnace for 10 min to saturate the environment with argon after which it was kept constant at 10 sccm.

Re-sulfurization of $MoOS_2$ crystals: A piece of growth substrate which contained $MoOS_2/MoS_2$ crystals was placed on top of a clean Si/SiO_2 substrate and placed them at the center of the furnace. 600 mg sulfur was placed upstream at a distance of 13 cm from the center of the furnace. Temperature was raised to 650 ^{0}C in a similar manner, hold for 10 min and allowed to cool down naturally. All other parameters kept the same as before.

Characterization of the materials

The surface imaging was carried out by Olympus BX51M microscope equipped with Jenoptic Progres Gryphax camera. The oxysulfide crystals were also imaged by Zeiss ULTRA-55 FEG SEM. A tapping mode AFM (Veeco instruments, Dimension 3100) topography was used to verify the height of the oxysulfide crystals and MoS_2 crystals. The samples were scanned at slow rates in small scan areas at the single crystal edge to achieve more accurate height profile. Raman and PL spectroscopy measurements were carried out with confocal Raman microscope (Witec alpha 300 RA) at excitation wavelength of 532 nm and power about 6.87 mW at ambient conditions.

RESULTS AND DISCUSSIONS:

Figure 2 show a representative growth results during CVD growth of MoS_2 after optimization of growth parameters. Concentration gradient of MoO_3 varies along the flow direction, therefore different crystals are grown on the substrate. Optical and SEM micrographs for commonly observed types of crystals are shown in figure 2 b), c), d) and e), f), g) respectively. In region 1, the substrate faces directly toward the MoO_3 powder and Mo vapor concentration is high resulting in square shaped $MoOS_2$ crystal growth. Further away from MoO_3 (region 2, figure 2c and 2f), we observed that triangular shaped MoS_2 is grown with thick nucleation as a result of moderately high Mo content[14, 15]. Further along the flow direction (region 3, figure 2d and 2g), monolayer MoS_2 single crystals have observed suggesting that ideal molar ratio of 1:3.5 between MoO_3 and S is maintained in this region. These results show that while MoS_2 single crystal can be obtained in certain part of the growth substrate, at other parts MoS_2 crystals grow along with $MoOS_2$ suggest a variation of vapor pressure along the flow direction.

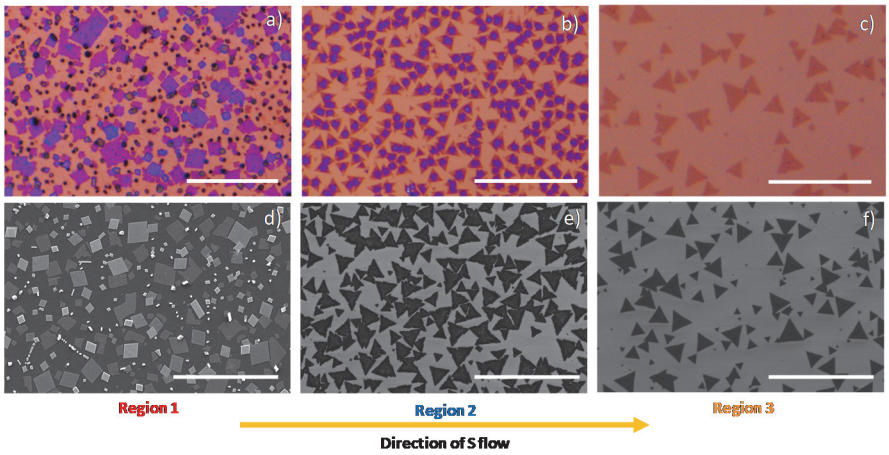

Figure 2. a), b), c) Optical micrographs and d), e), f) SEM images of crystals grown at different regions of the substrate with respect to the sulfur flow. The scalebar in each image is 25 µm.

Figure 3 shows Raman, PL and AFM characterization for these three regions. The square-shaped crystals grown in region 1 has Raman signature peaks at 130.32 cm^{-1}, 207.82 cm^{-1}, 233.95 cm^{-1}, 351.11 cm^{-1}, 365.52 cm^{-1}, 499.8 cm^{-1}, 573.69 cm^{-1}, 593.52 cm^{-1}, 745.82 cm^{-1} corresponds to $MoOS_2$[16]. It also shows E^1_{2g} and A_{1g} peaks at two MoS_2 signature peaks at 387.15 cm^{-1}, and 408.88 cm^{-1} with the spacing of $\Delta = 21.73$ cm^{-1} which corresponds to few layer MoS_2[15, 17]. Weak PL responses at 1.83 eV and 1.97 eV are observed from these crystals due to multilayer nature of MoS_2. Both Raman and PL spectroscopy data for the $MoOS_2$ crystals grown in region 1 suggests that they may contain MoS_2 at the surface. AFM height profile shows that these crystals can be as thick as 15.5 nm. The thick triangular domains in region 2 are characterized to be thick MoS2 with E^1_{2g} and A_{1g} Raman peaks at 388.95 cm^{-1} and 411.48 cm^{-1} ($\Delta = 22.53$ cm^{-1}) corresponding to a few layer MoS_2[15, 17]. PL spectra shows A (direct bandgap transitions) and B (excitations due to valence band splitting[18]) signature peaks at 1.85 eV and 1.99 eV with reduced intensity which also suggests the multilayer nature of these crystals. AFM measured thickness of 6.4 nm suggests they can be 9-10 layer thick MoS_2. Single crystals grown in region 3 has MoS_2 signature peaks at 389.86 cm^{-1} and 408.78 cm^{-1} with $\Delta = 18.92$

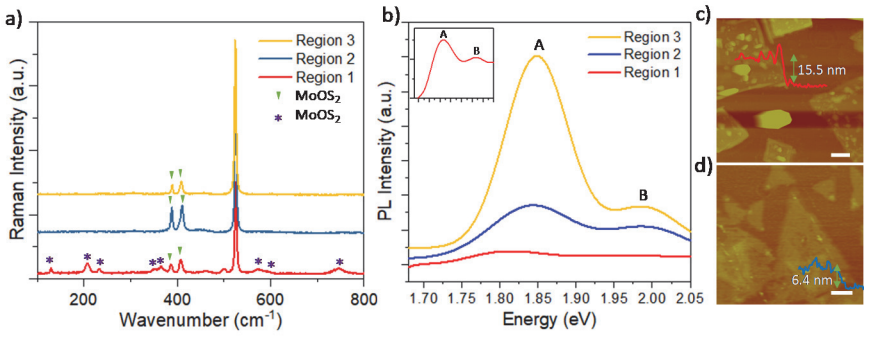

Figure 3. a) Raman spectrum taken at each region specified in figure 2. b) PL spectrum for the three regions. Zoomed in picture for the PL spectra for region 3 is shown in the inset of b). c), d) AFM topographies for the crystals grown in regions 1 and 2 respectively. The height profiles are provided in the insets.

cm^{-1} which is consistent with monolayer MoS_2[17, 19]. These monolayers also shows a very intense A peak at 1.85 eV in PL spectra which indicates direct bandgap transitions in monolayer[20, 21].

Figure 4 shows the results for re-sulfurization of $MoOS_2$ crystals in to MoS_2. We separated the region of a substrate where the oxysulfide crystals are grown and sulfurized it at 650 ^{0}C. The optical micrograph for after sulfurization result shown in figure 4b) by using 4a) as the source indicates that $MoOS_2$ crystals starts to grow in to MoS_2 around them, but due to high density of nucleation of these crystals hinder a clean MoS_2 growth after sulfurization. Then, we tested the resulfurization effect for a sample which contained moderate amount of $MoOS_2$ crystals along with MoS_2 (figure 4c). In contrast to 4b), 4d) shows that the oxysulfides were fully sulfurized to create MoS_2 in this sample under similar conditions. We measured the height of these MoS_2 crystals to be 0.9 nm using AFM topography which corresponds to the monolayer MoS_2 thickness. Δ=18.92 cm^{-1} between the Raman peaks and dominant A peak at 1.85 eV in PL intensity also confirm the monolayer nature of the MoS_2 crystals grown after resulfurization.

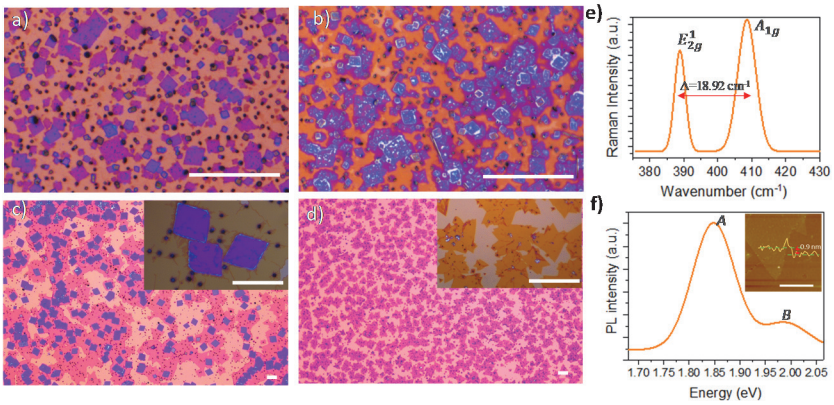

Figure 4. a), b) optical micrographs of before and after re-sulfurization results for dense $MoOS_2$ crystals. c), d) optical micrographs of before and after re-sulfurization results for $MoOS_2$ crystals with less coverage density grown along with MoS_2. Zoomed in images are shown in the insets. Scalebar for all optical images is 25 µm. e) Raman and f) PL spectrum for the crystals shown in d). The AFM topography and the height profile for the crystals is shown in the inset of f). Scalebar is 5 µm.

CONCLUSIONS

In summary, we demonstrate that different types of crystals can be grown during the CVD growth of MoS_2 due to local variations of vapor phase precursors. $MoOS_2$ are deposited in S deficient regions and we show that these crystals can be effectively sulfurized and transformed in to MoS_2 at moderate temperatures. Our study further elucidates MoS_2 growth mechanism during the CVD based co-evaporation technique. Resulfurization process we introduce here can be useful toward recycling of intermediate growth species in to reproducible growth of MoS_2

ACKNOWLEDGMENTS

This work was supported by U.S. National Science Foundation (NSF) under grants No. 1728309. We also acknowledge Dr. Tetard for Raman/PL spectroscopy support.

REFERENCES

1. N. Perea-López, A. L. Elías, A. Berkdemir, A. Castro-Beltran, H. R. Gutiérrez, S. Feng, R. Lv, T. Hayashi, F. López-Urías, S. Ghosh, B. Muchharla, S. Talapatra, H. Terrones and M. Terrones, Adv Funct Mater **23** (44), 5511-5517 (2013).
2. H. R. Gutiérrez, N. Perea-López, A. L. Elías, A. Berkdemir, B. Wang, R. Lv, F. López-Urías, V. H. Crespi, H. Terrones and M. Terrones, Nano Lett **13** (8), 3447-3454 (2013).
3. B. Radisavljevic, A. Radenovic, J. Brivio, V. Giacometti and A. Kis, Nat Nanotechnol **6** (3), 147-150 (2011).
4. O. Lopez-Sanchez, D. Lembke, M. Kayci, A. Radenovic and A. Kis, Nature Nanotechnology **8** (7), 497-501 (2013).
5. O. Salehzadeh, N. H. Tran, X. Liu, I. Shih and Z. Mi, Nano Lett **14** (7), 4125-4130 (2014).
6. D. Sarkar, W. Liu, X. J. Xie, A. C. Anselmo, S. Mitragotri and K. Banerjee, Acs Nano **8** (4), 3992-4003 (2014).
7. M. L. Tsai, S. H. Su, J. K. Chang, D. S. Tsai, C. H. Chen, C. I. Wu, L. J. Li, L. J. Chen and J. H. He, Acs Nano **8** (8), 8317-8322 (2014).
8. M. Li, J.-S. Chen, P. K. Routh, P. Zahl, C.-Y. Nam and M. Cotlet, Adv Funct Mater **28** (29), 1707558 (2018).
9. Y.-C. Lin, W. Zhang, J.-K. Huang, K.-K. Liu, Y.-H. Lee, C.-T. Liang, C.-W. Chu and L.-J. Li, Nanoscale **4** (20), 6637-6641 (2012).
10. A. E. Yore, K. K. H. Smithe, W. Crumrine, A. Miller, J. A. Tuck, B. Redd, E. Pop, B. Wang and A. K. M. Newaz, The Journal of Physical Chemistry C **120** (42), 24080-24087 (2016).
11. X. L. Li and Y. D. Li, Chem-Eur J **9** (12), 2726-2731 (2003).
12. J. V. Pondick, J. M. Woods, J. Xing, Y. Zhou and J. J. Cha, ACS Applied Nano Materials **1** (10), 5655-5661 (2018).
13. J. D. Cain, F. Y. Shi, J. S. Wu and V. P. Dravid, Acs Nano **10** (5), 5440-5445 (2016).
14. H. Zhou, C. Wang, J. C. Shaw, R. Cheng, Y. Chen, X. Huang, Y. Liu, N. O. Weiss, Z. Lin, Y. Huang and X. Duan, Nano Lett **15** (1), 709-713 (2015).
15. D. Zhou, H. B. Shu, C. L. Hu, L. Jiang, P. Liang and X. S. Chen, Cryst Growth Des **18** (2), 1012-1019 (2018).
16. V. Senthilkumar, L. C. Tam, Y. S. Kim, Y. M. Sim, M. J. Seong and J. I. Jang, Nano Res **7** (12), 1759-1768 (2014).
17. C. Lee, H. Yan, L. E. Brus, T. F. Heinz, J. Hone and S. Ryu, Acs Nano **4** (5), 2695-2700 (2010).
18. J. Zhang, H. Yu, W. Chen, X. Z. Tian, D. H. Liu, M. Cheng, G. B. Xie, W. Yang, R. Yang, X. D. Bai, D. X. Shi and G. Y. Zhang, Acs Nano **8** (6), 6024-6030 (2014).
19. A. Sanne, R. Ghosh, A. Rai, M. N. Yogeesh, S. H. Shin, A. Sharma, K. Jarvis, L. Mathew, R. Rao, D. Akinwande and S. Banerjee, Nano Lett **15** (8), 5039-5045 (2015).
20. K. F. Mak, C. Lee, J. Hone, J. Shan and T. F. Heinz, Phys Rev Lett **105** (13) (2010).
21. N. Choudhary, M. R. Islam, N. Kang, L. Tetard, Y. Jung and S. I. Khondaker, J Phys-Condens Mat **28** (36) (2016).